

External Command Study of the Phase Shifter for Applications to Array Antenna with Nematic Liquid Crystal

A. Attoui*, H. Boualleg

*Laboratory for Telecommunications(LT)
Faculty of Science and Technology
University May 8, 1945 Guelma, Algeria
Email: atoui.aissa@gmail.com*

Abstract

This article is devoted to characterization by finite difference method in simulation software HFSS of Coplanar microwave phase shifter based on liquid crystal for array antenna printed electronic scanning. In this paper we propose a new external Phase Shifter command. The structure consists of three parts of liquid crystal placed between the ground plane and transmission line. The simulation results concerning the losses in reflection of phase shifter and the influence of the static magnetic bias field of liquid crystal on these parameters are shown in detail.

Keywords: COPLANAR LC PHASE-SHIFTER, LIQUID CRYSTAL, ARRAY ANTENNA, EXTERNAL COMMAND, FINITE DIFFERENCE METHOD

Introduction

Beam-steering antennas are the ideal solution for a variety of system applications including traffic control,[1] regulation and collision avoidance radars installed on most ocean going ships to provide better detection of ships in rough sea and heavy rain condition. Beam-steering antennas also used in smart base station antennas for WLAN and cellular communication [1][2]. Beam-steering is most commonly achieved through phased arrays, where phase shifters are used to control the relative main-beam of the antenna array. Many antenna system applications require that the direction of the beam's main lobe was changed with time, or scanned.

In the last decade, liquid crystals (LC) have been investigated as active dielectric for tunable microwave devices [3]. This represents a new application of these materials largely used in visualization displays. Liquid crystals were used to realize tunable phase shifters,

planar antennas and filters [3][4]. LC present good potentialities among them, low driving electric field (typical $0.2\text{V}/\mu\text{m}$) and relatively low.

Operation of these phase shifters is based on controlling the orientation of LCs anisotropy of dielectric permittivity with an applied electric field, which allows for external control of the phase of microwave signal. It is well known that when the relative phases of the feeding RF signals to the array antenna are changed, the direction of a main beam can be controlled [4]. Thus in our experiment, a LC loaded phase shifter which we had fabricated is used to control electrically the phase of the feeding RF signal.

This is usually done by mechanically rotating a single antenna or an array with fixed phase to the element. However, mechanical scanning requires a positioning system that can be costly and scan too slowly. For this reason, electronic scanning antennas, which are known as phased array antennas, are used. It can

sweep the direction of the beam by varying electronically the phase of the radiating element, thereby producing a moving pattern with no moving parts. Phased array antennas are the fundamental function of a phase shifter circuit is to produce a replica of the signal applied at its input [1], but with a modified

phase. The general structure of an antenna network with electronic scanning is shown schematically in Figure 1. The use of the liquid crystal allows integrating the phase shifter and the change in phase of the signal is obtained by the action of the static magnetic field applied to the liquid crystal.

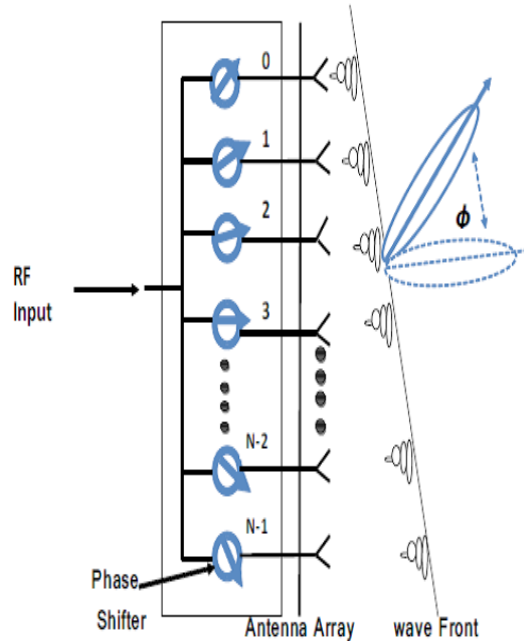


Figure 1. Phased array antenna

Nematic Liquid Crystal

Here we present LC. Under the applications we use the LC nematic phase in an ambient temperature [2][5]. The nematic LCs are characterized by their center of gravity, the molecules showing no order of position. However, molecules procure an orientation

order in case of long distance [6]. Their long-distance and long axes are parallel to an average direction defined by the vector director n (Figure 2). In this phase the LCs are anisotropic materials with complex permittivity presented in the form of a tightening (equation 1)[1][5].

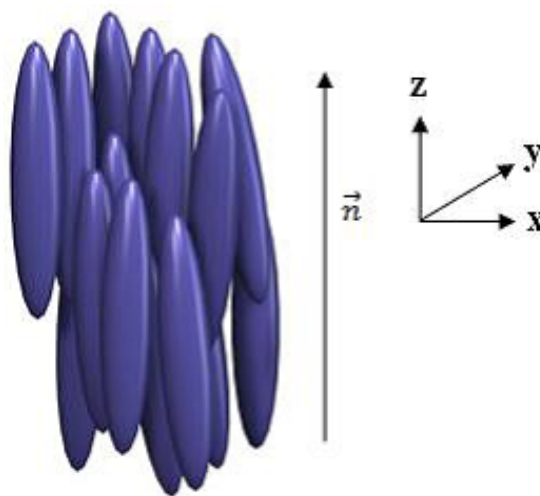


Figure 2. Representation of molecules CL in phase Nematic

$$\epsilon^* = \begin{bmatrix} \epsilon_{\parallel}^* & 0 & 0 \\ 0 & \epsilon_{\perp}^* & 0 \\ 0 & 0 & \epsilon_{\perp}^* \end{bmatrix}$$

(1)

It then defines the dielectric anisotropy by the equation 2.

$$\Delta\epsilon = \epsilon_{\parallel}^* - \epsilon_{\perp}^* \tag{2}$$

$\Delta\epsilon$: Dielectric anisotropy
 ϵ_{\square} : LC permittivity with DC voltage
 ϵ_{\perp} : LC permittivity without DC voltage

Measures in two different directions of the material are needed to determine each of its parameters [2],[6]. It is possible to orient the liquid crystal by applying an outside magnetic field of typical 0.4 Tesla. Therefore the molecules align their long axis in its direction.

The permittivity analyzed by the microwave field E_{HF} measure amends following this trend.

Here we will choose two configurations in the measurement of permittivity ϵ_{\square} and ϵ_{\perp}

Studied Materials

The LC is the simulated K15 (5cb) (pentylcyano-

biphenyl) which exhibits only nematic phase between 22.5° and 35° . This figure shows the dielectric characterization of K15 at room temperature [7].

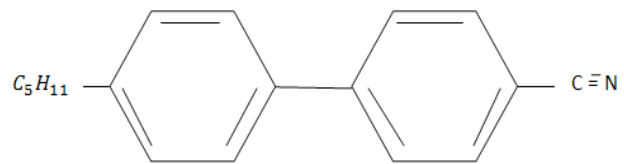


Figure 3. Chemical formula of liquid crystal K 15

The characteristics of liquid crystals are summarized in Table 1.

Table 1. Characteristics of liquid crystal

CL	sequence phase	ϵ'_{\perp}	$\tan \delta_{\perp}$	ϵ'_{\square}	$\tan \delta_{\square}$	$\square \epsilon'$
5CB	C 22.5°	2.64	0.031	2.98	0.014	0.34
	CN 35° CI					

Phase Shifter agile Frequency Liquid Crystal Substrate

Order of liquid crystal within a microwave substrate In the case of a line micro strip classic, the gap reached between input and output is fixed at a given frequency [2]. This phase shift depends on effective permittivity and the line length of the following:

$$Q = \frac{360.L.F.\sqrt{\epsilon_{reff}}}{c} \tag{3}$$

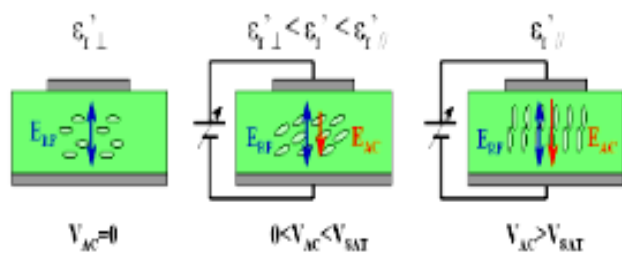


Figure 4. Influence of an electric field command on the orientation of liquid crystal

The electrodes by treating surface (planar orientation) [2]. The permittivity seen by the microwave signal is noted $\epsilon_{reff(0)}$.

This permittivity is related mainly to the permittivity LC $\epsilon_{r\perp}$.

As a result of the electric field command, the molecules of LC will gradually move perpendicular to the electrodes (n/E) to saturation permittivity. The east

view $\epsilon_{reff(E)}$.

The saturation permittivity $\epsilon_{reff(E)}$ is related mainly to the liquid crystal permittivity $\epsilon_{r\square}$.

This variation of permittivity will induce a change in the wavelength guided; [2] therefore a change in phase is given by:

$$\Delta Q = \frac{-360.L.F.(\sqrt{\epsilon_{reff(E)} - \epsilon_{reff(0)}})}{c} \tag{4}$$

Phase Shifter Design

In a first step, the HFSS (High frequency structure simulator), designed phase shifter.

The structure of the phase shift is shown in figure 5. The two illustrations (figure 6, and 7) show the two parts of the circuit component. The figure 6 a coplanar line is a structure in which all the conductors supporting wave propagation are located on the same plane.

The figure 7 consists of a brass plate in which a cavity, which serves to confine the LC, is grave. This cavity is positioned at the active portion of the circuit. The assembly of these two parts provides the final structure for coplanar phase shifter illustrated in Figure5.

Results and discussions

The simulation results are created by the simulator HFSS, for the applicability of the 3 crystal liquid parts proposed.

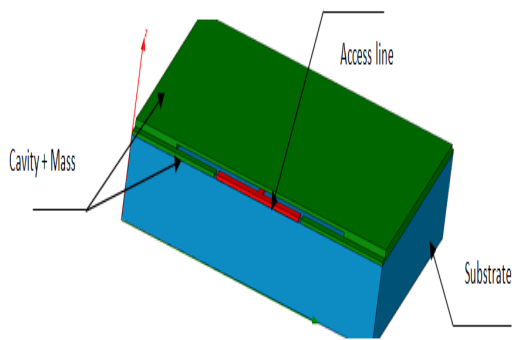


Figure 5. Structure of coplanar phase shifter

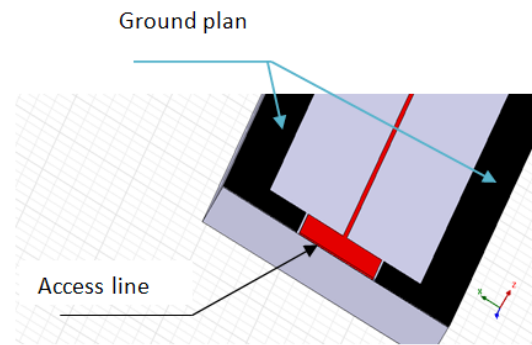


Figure 6. (CPW)

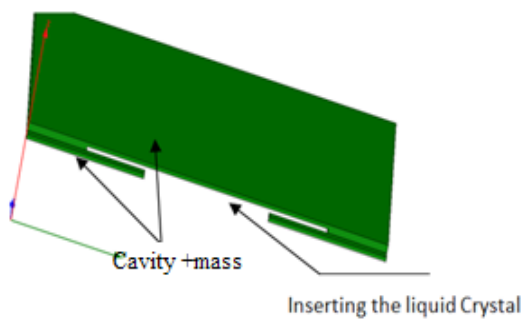


Figure 7. Cavity +mass

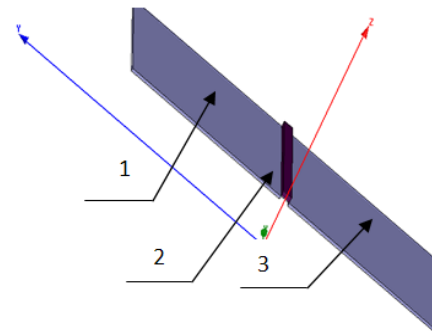


Figure 8. The 3 LC parts

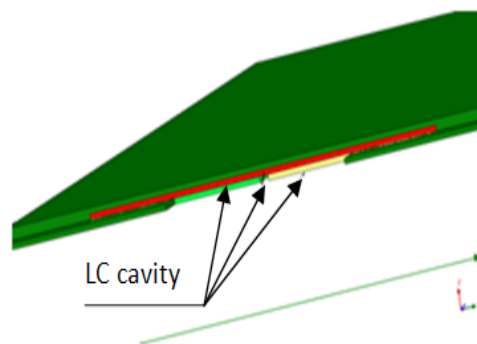


Figure 9. LC cavity position

The simulation is performed in the frequency range (10 – 50GHz) to obtain the phase-shifter characteristics. The substrate is realized by DUROID 4003. The dimensions of the phase shifters active part are the following: (X size 3.06 mm, Y size 15 mm, and Z size 0.05 mm). The liquid crystal is introduced between the ground plane and the transmission lines with dimensions are the following: part 1 and 3 (X

size 1 mm, Y size 14 mm, and Z size 0.025 mm) and part 2 (X size 0.05 mm, Y size 14 mm, and Z size 0.025 mm) The amplitude of the reflection coefficients versus frequency of the phase shifter is given in Figures 10. Without driving, a good matching of the device is observed ($S_{11} < -30$ dB). The phase of (S_{21}) for different excitations is shown in figures: 11, 12 and 13.

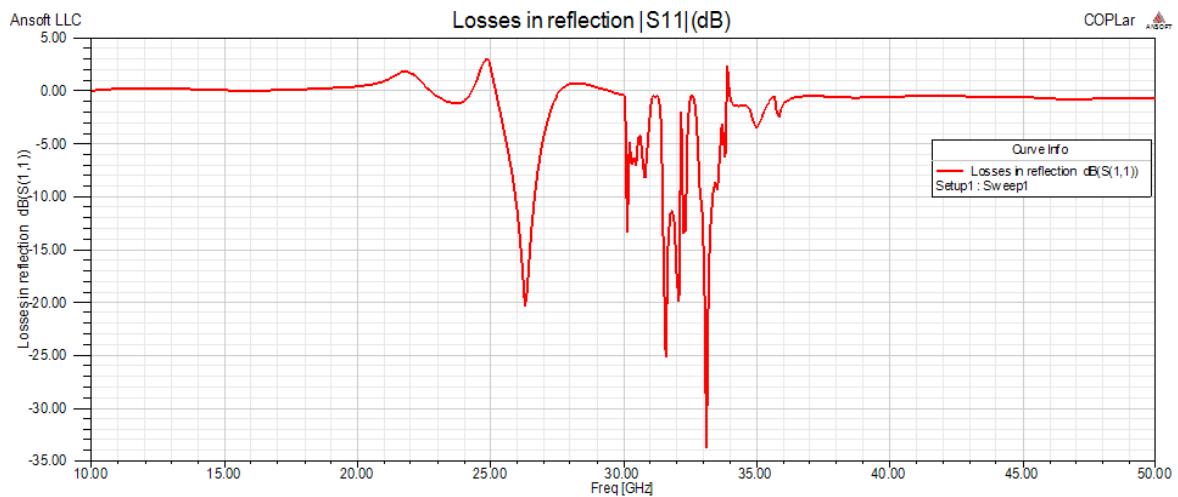


Figure 10. The reflection coefficients S11 (dB) of the phase shifter

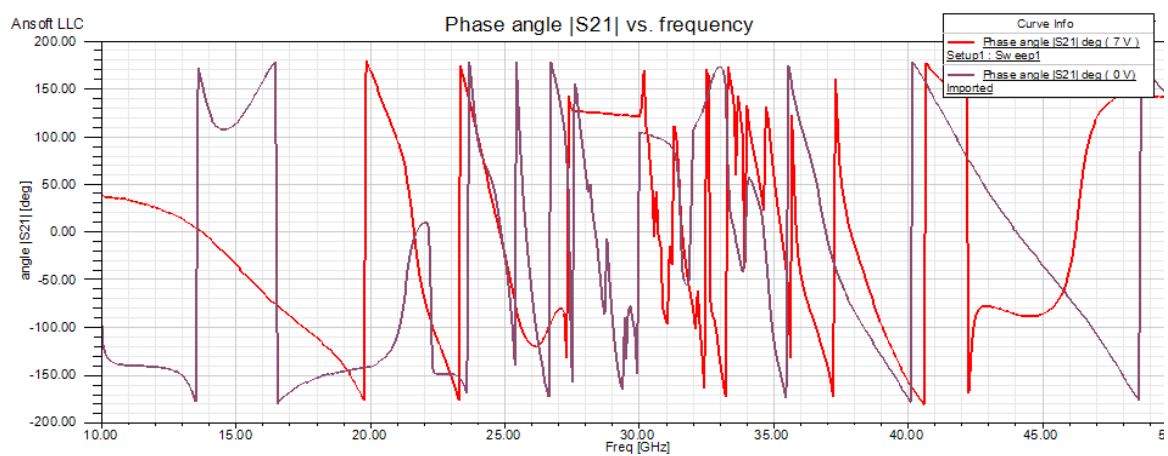


Figure 11. Phase angle |S11| (degree) of phase shifter, with and without control voltage

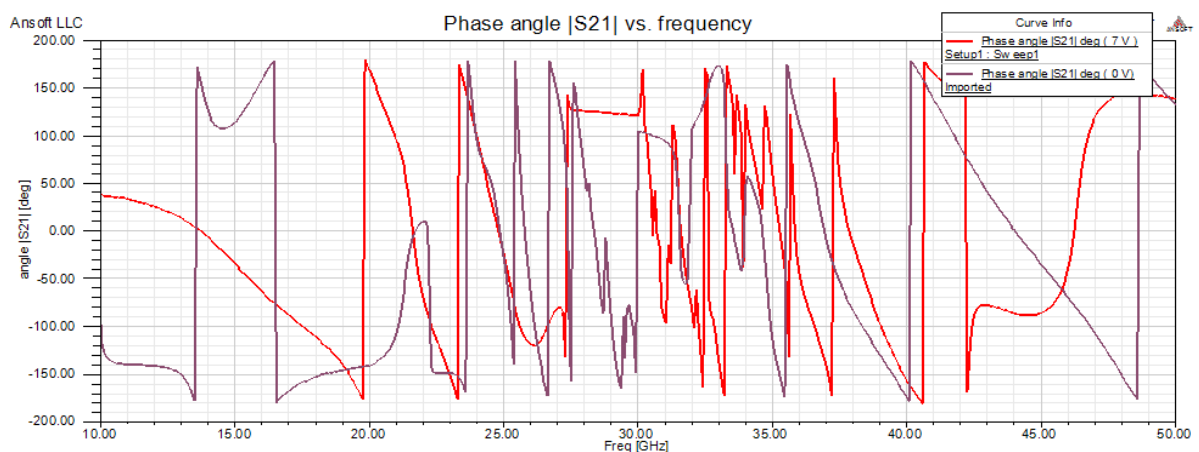


Figure 12. Change phase S (21) (degree) of phase shifter depending on the frequency, with and without Control voltage

The (S21) phase variations as a function of frequency are given in Figures 11. The (S21) phase variation is calculated from the difference between the (S21) phase measured with and without driving voltage (0 V and 7 V). The (S21) phase evolves linearly with frequency. At 30 GHz, the value of the phase angle |S11| variation is approximately 20°

Figure 13, shows the phase shift obtained from the excitations positions we give the (S21) phase variation evolution versus excitation position. The structure is composed of three parts of liquid crystal placed between the ground plane and the transmission line (part 1, 2 and 3).

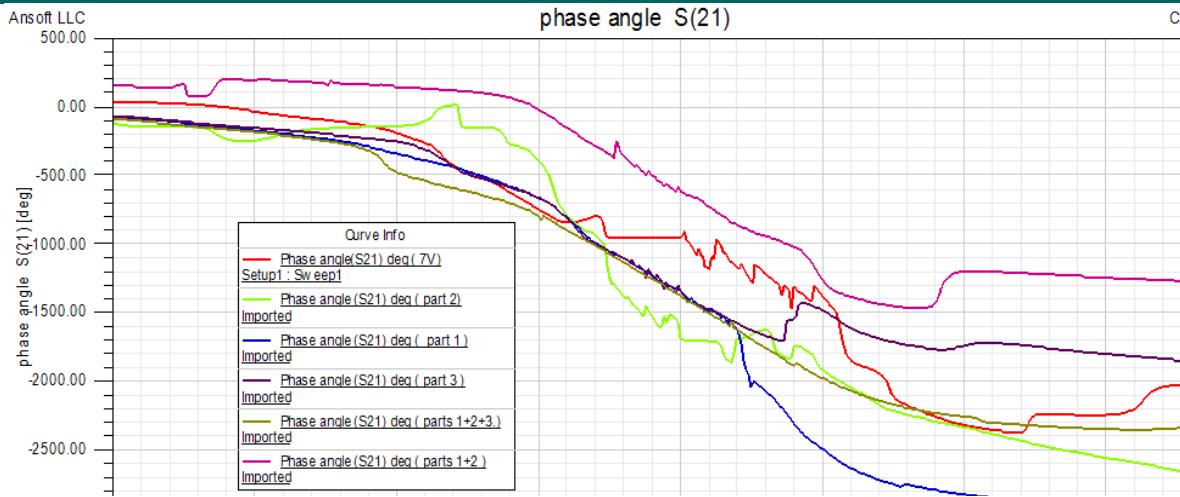


Figure 13. Change phase (S21) (degree) of phase shifter depending on the frequency, taking part 1, 2, and 3

This figure show a comparison between the phases results obtained of (S21) for different excitations parts ((degree) of phase shifter).

The approximate values of the phase variation obtained at 35 GHz taking parts 1, 2, and 3, shown in table 2

Table 2. Phase shift obtained at 35 GHz taking part1, 2, and 3

comparison	part1	part3	part1 + 2 + 3
part1	24	100°	50°
part2	60°	40°	10°
part1 + 2	120°	20°	70°

Conclusion

In this paper we describe a study on phase shifter based on liquid crystal. The proposed method was based on two influences (voltage and position) on the phase of the transmission coefficient (S21) with HFSS software. Obtained results reveal that we can control the phase shift with the excitation voltage and in addition the position of excitation. In the present work, we proved that is possible to control phase shifter with a new standard that is the position of excitation.

References

1. Puneet Anand, Sonia Sharma, Deepak Sood, C.C.Tripathi. Design of compact reconfigurable switched line microstrip phase shifters for phased array antenna. (ET2ECN), 2012 1st International Conference , Vol. 1 - 3, No. 978-1-4673-1627-9/12/31.00 A c 2012 IEEE.
2. Sahbani, F., L. Emcel, Tentillier N., Gharsallah A., Gharbi A. New tunable coplanar microwave phase shifter with nematic crystal liquid. IEEE, Design and Test Workshop, 2008. IDT

2008. 3rd International , 78 - 81, No. 978-1-4244- 3477-0/08/25.00 A c 2008 IEEE.
3. F. Sahbani, N. Tentillier, C. Legrand, K. Blaary, A. G. Harsallah, A.Gharbi. Coplanar Liquid Crystal Reconfigurable Phase-Shifters. *Journal of Molecular Crystals and Liquid Crystals*, Vol. 542, p.p. 204, 2011.
4. T. Kamei, M. Yokota, R. Ozaki, H. Moritake, N. O Nodera. Microstrip Array Antenna with Liquid Crystals Loaded Phase Shifter. *Journal of Molecular Crystals and Liquid Crystals*, Vol. 542, p.p. 167.
5. Missaoui, S., Gharbi, A., Kaddour M. (2011). Design and simulation reconfigurable liquid crystal patch antennas on foam substrate. *Journal of Chemical Engineering and Materials Science*, Vol. 2(7), No. p.p. 96-102.
6. Christian Weickhmann, Norbert Nathratha, Ralf Gehringa, Alexander Gaeblera, Matthias Josta, Rolf Jakobya. A Light-Weight Tunable Liquid Crystal Phase Shifter for an Efficient Phased Array Antenna. *Microwave Conference (EuMC), 2013 European* , p.p. 428 – 431.
7. Carsten Fritzscha, Flavio Giacomozzi, Onur Hamza Karabey, Felix Goelden, Alexander Moessinger, Saygin Bildik, Sabrina Colpo, Rolf Jakoby. Continuously Tunable W-Band Phase Shifter based on Liquid Crystals and MEMS Technology. *Proceedings of the 6th European Microwave Integrated Circuits Conference.*, 978-2-87487-023-1 A c 2011 EuMA
8. Manish , Puri Anamika , Das Jitendra , Singh Sengar. A Novel Design of Monolithically Integrated Phased Array Antenna Employing 4-bit DMTL Phase Shifter. *Wireless and Optical Communications Networks (WOCN), 2013 Tenth International Conference on*, 1 - 6,

- No.978-1-4673-5999-3/13/31.00 Ac 2013 IEEE.
9. Belyaev B. A., Leksikov A. A., Serzhantov A. M., Shabanov V. F. (2008). Controllable Liquid-Crystal Microwave Phase Shifter. *TECHNICAL PHYSICS LETTERS*, Vol. 34 No 6.
 10. Z.M. Huang, D.Y. Zhang, Y.Q. Luo, J.F. Li, C.L. Liu. A new configuration for phase control in laser coherent combination utilizing liquid crystal optical modulator. *Applied physics*, Ac Springer, Verlag 2010.
 11. B. T. P. Madhav, VGKM Pisipati, N. V. K Ramesh, Habibulla Khan, P. V. Datta Prasad, "PLANAR INVERTED-F ANTENNA ON LIQUID CRYSTAL POLYMER SUBSTRATE FOR PCS, UMTS, WIBRO APPLICATIONS," *ARPJ Journal of Engineering and Applied Sciences*, Vol. 6, No 4, APRIL 2011.
 12. F. A. Tahir, H. Aubert "EQUIVALENT ELECTRICAL CIRCUIT FOR DESIGNING MEMS-CONTROLLED REFLECTARRAY PHASE SHIFTERS" *Progress In Electromagnetics Research*, PIER,100, 1^a^12, 2010.
 13. Zhou Du, Ville Viikari, Juha Ala-Laurinaho, Aleksi Tamminen, Antti V. R. A^ais A anen. Antenna Pattern Retrieval from Reflection Coefficient Measurements with Reflective Loads. *Progress In Electromagnetics Research*, PIER, Vol. 148, 15 a 22, 2014
 14. Z. G. Wang, B. Yan, R. M. Xu, and Y. C. Guo "Design of a KU band six bit phase shifter using periodically loaded-line and switched-line with loaded-line" *Progress In Electromagnetics Research*, PIER,76, 369 a^379, 2007.



Wellbore Temperature Distribution in Hydraulic-Fracturing Horizontal Wells for Gas

Junjun Cai*, Yonggang Duan

State Key Laboratory of Oil and Gas Reservoir Geology and Exploitation, Southwest Petroleum University, Chengdu 610500, Sichuan, P.R. China

Abstract

Use of distributed temperature sensors (DTS) to monitor the productive zones of horizontal wellbores by real-time temperature profile measurement is becoming an industry standard. Well completion method, skin factor and non-Darcy flow phenomenon are among operating parameters potentially related to DTS data. In order to study on the above-mentioned relationship, this paper establishes temperature models which consider skin factor and non-Darcy flow, in turn whose foundation are mass-, momentum-, and energy-balance equations. The models presented here account for heat convection, fluid expansion, heat conduction and viscous dissipative heating. Once configured, these models were applied to predict wellbore temperature distribution and analyze factors influencing the wellbore temperature profile. Arriving temperature and wellbore temperature curves are plotted by